Optical Materials: X 1 (2019) 100001

Contents lists available at ScienceDirect

Optical Materials: X

journal homepage: www.journals.elsevier.com/optical-materials-x

On thermoluminescence mechanism and energy leakage in Lu_2O_3:Tb,V storage phosphor

Justyna Zeler, Paulina Bolek, Dagmara Kulesza, Eugeniusz Zych*

Faculty of Chemistry, University of Wroclaw, 14. F. Joliot-Curie Street, 50-383, Wroclaw, Poland

ARTICLE INFO

Keywords:
Storage phosphors
Lutetium oxide
Semi-localized transition model
Continuous distribution of trap energy

ABSTRACT

The energy storage properties of Lu_2O_3:Tb,V sintered materials when exposed to X-rays were investigated for the first time using a number of thermoluminescent techniques. Thermoluminescence was generated exclusively by the Tb^{3+} ions, which served also as hole-trapping centers. Two TL peaks at ~170 °C and 220 °C were found to be directly connected with V-electron traps and were assigned to the release of first (170 °C) and second (220 °C) electron from V_{Lu}^{X}. It was evidenced that each of the two TL bands results from strongly overlapping components showing continuous distribution of energies. Significant contribution from semi-localized transitions to carriers annihilation was also proved.

1. Introduction

Research on rare earth-doped Lu_2O_3 phosphors was pretty intense in last twenty years [1–8]. It was mainly related to scintillators/X-ray phosphors, up-converters, lasers, and persistent luminescence or energy storage phosphors. The last two were found especially efficient if activated with Tb or Pr and co-activated with aliovalent dopants: Ca/Sr/Ba (for persistent emission) or Ti, Hf, Nb, Ta (for permanent energy storage in deeper traps) [4,8–20].

The undertaken research allowed to understand many aspects of the mechanism of energy storage and subsequent controlled release by thermal or optical stimulation in these materials. Yet, the understanding of some details of the processes related to energy storage is still elusive. Besides, new compositions showing ability for carriers trapping are reported repeatedly. This also applies to the Lu_2O_3:Tb,V ceramics reported here.

It was concluded that hole trapping in these materials is describe by Eq. (1)

$$Tb_{Lu}^{\times} + h^{\cdot} \rightarrow Tb_{Lu}^{\cdot}, \quad (1)$$

proving that Tb^{3+} (or Pr^{3+}) is directly involved in this process. More recently, it was accepted that electrons trapping occurs by their localization at the co-dopants' (Hf, Ti, Nb, Ta) empty orbitals as schematically exemplified in Eq. (2) [3,8,21].

$$M_{Lu}^{\cdot} + e' \rightarrow M_{Lu}^{\times} \quad (2)$$

Then, the final states after the carriers trapping are Tb^{4+} and Ti^{3+}/Hf^{3+}, in principle. In the case of co-doping with Nb/Ta two TL peaks clearly related to these impurities were systematically observed and were assigned to Ta/Nb traps filled with one ($Ta_{Lu}^{\cdot}$) or two ($Ta_{Lu}^{\times}$) electrons [3,6,8,21]. Those conclusions accord with the recent developments of the Dorenbos semi-empirical model [22–25].

In this paper we present TL properties of the Lu_2O_3:Tb,V ceramics for the first time. A set of thermoluminescent experiments shall be presented to expose the traps structure and learn on the processes of energy storage and release in this material.

2. Experimental section

Lu_2O_3:Tb,V materials were prepared in the form of ceramic pellets ~8 mm in diameter and about 0.5 mm thick. The samples surfaces were ground and mirror-polished before measurements. Concentration of the V co-dopant was in the range of 0.05–0.2 mol% and that of Tb was fixed at 0.1 mol%. The sintering was performed at 1700 °C for 5 h in reducing atmosphere of N_2-H_2 (75%–25%) mixture. Some samples were prepared in air for comparison. The powders for sintering were synthesized by means of Pechini method [26]. More details on the synthesis and sintering can be found in papers published previously [2,3,6,8,18,21].

Crystallographic purity of all investigated compositions was tested by means of powder X-ray diffraction (XRD) method using a D8 Advance diffractometer from Bruker with Cu Ka_1 radiation of 1.54060 Å wavelength. TL glow curves, TL luminescence spectra and isothermal decay traces (ITDs) were recorded using Lexsygresearch Fully Automated TL/OSL Reader from Freiberg Instruments GmbH. It

* Corresponding author.
E-mail address: eugeniusz.zych@chem.uni.wroc.pl (E. Zych).

https://doi.org/10.1016/j.omx.2018.100001
Received 9 November 2018; Accepted 26 November 2018
Available online 07 December 2018

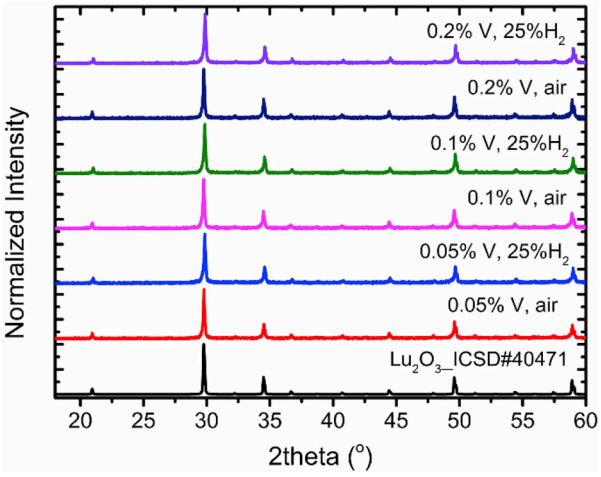

Fig. 1. The representative XRD patterns of the Lu_2O_3:0.1%Tb,x%V sintered ceramics fabricated in indicated atmospheres together with a simulated diffraction pattern of the cubic structure of Lu_2O_3 (#ICSD 40471).

used Varian VF-50J RTG X-ray lamp with W-anode which operated under 30 kV and 0.1 mA. The TL glow curves and isothermal decays (ITDs) were collected with a 9235QB-type photomultiplier from ET Enterprises. TL spectra were recorded with an Andor DU420A-OE CCD Camera electronically cooled to −80 °C. All experiments were controlled by means of LexStudio 2 software and resultant data were processed under LexEva 2 analytical software dedicated to the TL/OSL Reader and supplied by the manufacturer. Deconvolution of glow curves was executed using the Glowfit software [27].

3. Results and discussion

3.1. Structural analysis

In Fig. 1 the representative XRD diffraction patterns of the Lu_2O_3:0.1%Tb,x%V (x = 0.05–0.2) sintered materials are shown together with a simulated pattern of the cubic C-type structure of Lu_2O_3 [28,29]. The results confirmed that fabricated ceramics were phase pure and the dopants dissolved in the host.

3.2. Thermoluminescence

In Fig. 2a the TL glow curves of X-ray irradiated Lu_2O_3:0.1%Tb,x%V (x = 0.05–0.2) ceramics are presented. The samples were fabricated in different atmospheres at 1700 °C. It should be mentioned that TL intensity increases with temperature processing which is a common property of the Lu_2O_3-based storage phosphors [3,6,8,18]. The most efficient TL was observed for samples prepared in reducing atmosphere and for low (0.05 mol%) concentration of V.

Two TL peaks were systematically observed at ~170 °C and ~220 °C, see Fig. 2a. Their positions were independent on the co-dopant content and of the processing atmosphere proving that in all cases the same type of traps contributed to TL. For higher V concentrations (0.1–0.2%) the TL efficiency decreased very quickly and it virtually disappeared at V content of 0.2%, see Fig. 2a. Depending on the sintering atmosphere only small change in relative intensities of the two TL peaks was observed. Despite the two main peaks a low-intensity TL appeared around 90 °C. This component was routinely observed in most TL glow curves of Lu_2O_3:Tb-based ceramics and has intrinsic character [8].

Fig. 2b proves that the TL is produced exclusively by the Tb^{3+} activator with the main emission features around 540 nm ($^5D_4 \rightarrow {}^7F_5$ transition) and 480 nm ($^5D_4 \rightarrow {}^7F_6$) and less intense groups of lines in the range of 575–700 nm ($^5D_4 \rightarrow {}^7F_{4\text{-}0}$). Hereafter, thermoluminescent data were collected on the most efficient Lu_2O_3:0.1%Tb,0.05%V ceramics sintered in reducing atmosphere.

In Fig. 3 the TL glow curves of Lu_2O_3:0.1%Tb,0.05%V as a function of X-ray irradiation time (dose) are presented. The TL intensity increases with the dose but the peak positions are firmly stable. This indicates a first order kinetics of the TL process [30]. Around 330 °C a low-intensity component was systematically observed. Its relative intensity increased significantly for the highest dose. Studying it was beyond the scope of this research, however.

A rough estimation of the number of traps involved in the energy trapping can often be obtained by deconvolution of the experimental glow curves [31–33]. The results are presented in Fig. 3b for the Lu_2O_3:0.1%Tb,0.05%V ceramics. Five components were needed to get a good quality fit. While the shallowest intrinsic trap (grey line in Fig. 3b) contributes only insignificantly to the total TL, the other 4 (V-related) components are all substantial, and are clearly connected with V impurity. The obtained trap depths, E, with values in the range of 1.15–1.35 eV and relative frequency factors, s, very close to $1.7*10^{13}$ s^{-1} – a theoretical value for the Lu_2O_3 host whose most energetic phonons have the energy of 580 cm^{-1} [34] - are listed in Table 1 and in Fig. 3b. The very good quality of the fit (FOM = 1.2%) implies that each of the two main TL experimental strongly overlapping peaks may indeed comprise two individual strongly overlapping components. This, however, shall be critically verified by experiments discussed below.

Two types of experiments are typically recommended in tracing strongly overlapping individual TL components. First of them is based

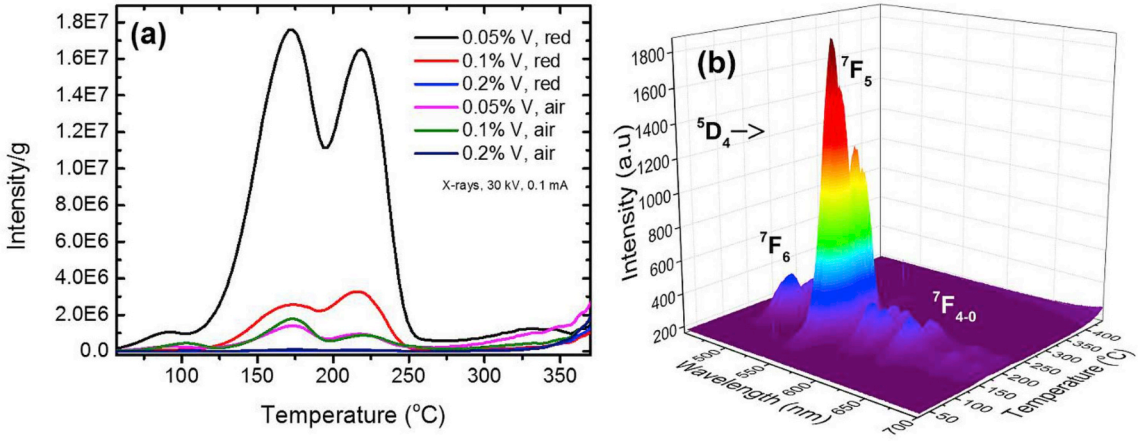

Fig. 2. (a) The TL glow curves of X-ray irradiated Lu_2O_3:0.1%Tb,x%V materials sintered at indicated atmospheres. (b) 3D temperature- and wavelength-resolved thermoluminescence of Lu_2O_3:0.1%Tb,0.05%V sintered in reducing conditions.

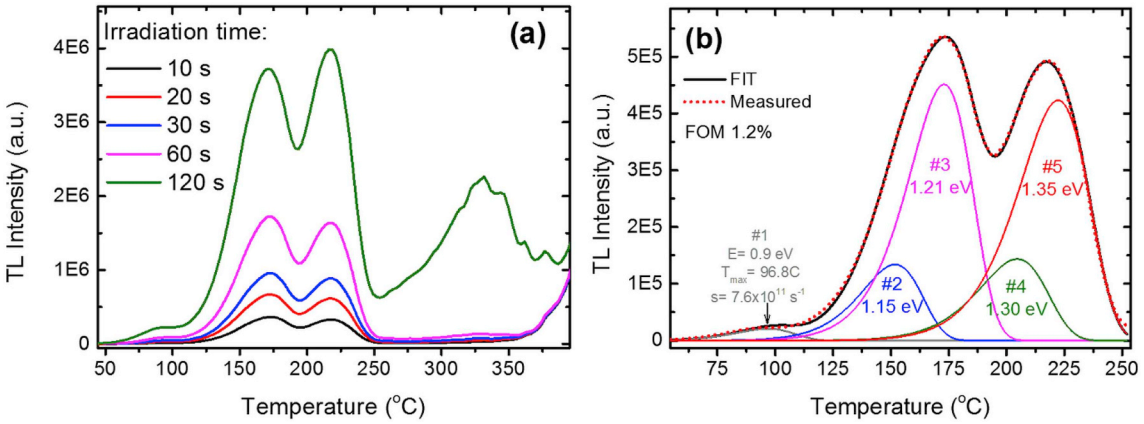

Fig. 3. (a) Dependence of the glow curves of Lu_2O_3:0.1%Tb,0.05%V on the X-ray dose (10–120 s). The glow curves were corrected for thermal quenching of the Tb^{3+} luminescence [8]. (b) Glow curve of Lu_2O_3:0.1%Tb,0.05%V ceramics and its deconvolution into five components. See also Table 1.

Table 1
Parameters of traps derived by deconvolution of the experimental glow curve of Lu_2O_3:0.1%Tb,0.05%V prepared in reducing atmosphere. Traps numbering as in Fig. 3b. FOM = 1.22.

Trap	T_m (°C)	E (eV)	s (s^{-1})	Trap lifetime (h/years)
Trap #2	151.8	1.15	$1.6*10^{13}$	488/-
Trap #3	172.9	1.21	$1.7*10^{13}$	4751/0.54
Trap #4	204.6	1.30	$1.7*10^{13}$	158076/18
Trap #5	222.3	1.35	$1.8*10^{13}$	1046000/120

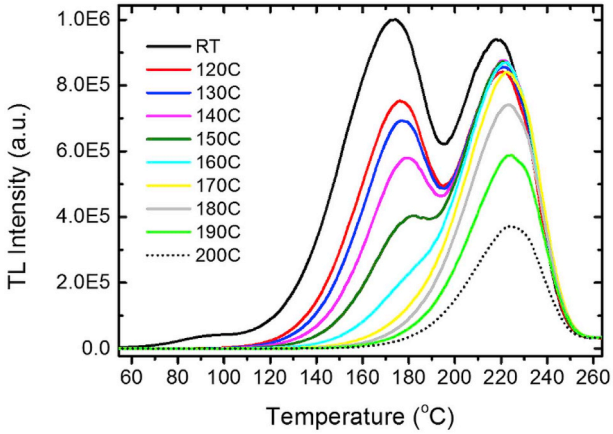

Fig. 4. The TL glow curves of Lu_2O_3:0.1%Tb,0.05%V ceramics after irradiation with X-rays at the indicated temperatures.

on TL glow curves measured after irradiation of the material under investigation at different temperatures and the other one is termed T_{max}-T_{stop} measurement [35–37]. Figs. 4 and 5 presents results of such experiments for the Lu_2O_3:0.1%Tb,0.05%V ceramics.

From Fig. 4 it is obvious that with increasing temperature of irradiation the glow curve gets narrower continuously losing its lower temperature part. Simultaneously, both TL peaks shift *steadily* to higher temperatures. This may indicate that both TL components are actually composed of many individual TL peaks due to continuous distribution of trap energies [33,35,38]. Irradiation at 170 °C leaves only the higher temperature TL peak. Its position also shifts continuously to higher temperatures as the irradiation temperature further increases.

In Fig. 5a the results of T_{max}-T_{stop} measurement are presented. The continuous shift of both TL peaks with increasing T_{stop} is perfectly evident from Fig. 5a. However, the detailed T_{max}-T_{stop} dependence presented in Fig. 5b shows that each of the two main TL peaks actually consist of a low intensity trap with a well-defined energy/depth (the flat parts of the T_{max}-T_{stop}, traps #2 and #4) and much more intense component composed actually of a set of traps with continuous distribution of energies (#3 and #5) [36–38]. The continuous distribution of trap energies is at first puzzling taking into account the very good quality of TL glow cure fit (deconvolution) presented in Fig. 3 and Table 1 with practically theoretical value of the frequency factor (see Table 1). We shall return to this problem discussing fading and heating rate-dependence of glow curves.

Next, room temperature fading of the TL signal and isothermal decays were measured to learn more about the mechanism of carriers releasing/time stability of their trapping. According to Arrhenius Eq. (3):

$$p = \tau^{-1} = s\mathrm{e}^{-\frac{\Delta E}{kT}}, \quad (3)$$

where p is the rate of a trap depopulation, τ is the trap lifetime, s is frequency factor, DE is the trap depth, k is Boltzmann constant and T stands for temperature in Kelvins the lifetimes for the traps #2–5 were calculated and are listed in last column of Table 1. Generally, the lifetimes are long (Trap #2) or very long. The measurements of the TL signal fading critically verified these predictions.

Fig. 6a presents changes in TL glow curves within the first 10 h after exposure of the material to X-rays. It is immediately seen that the fading is significant and both TL peaks related to V co-dopant decrease in intensity substantially and continuously. The ~170 °C component decays faster but the ~220 °C TL peak reduces its intensity only slightly slower. Evidently, the experimental fading is by far more potent than predicted by the Arrhenius equation using the estimated parameters of traps (see Table 1 and Fig. 3b). This infers that the de-trapping process in the Lu_2O_3:Tb,V ceramics is governed by more complex - conceivably mixed - mechanism, and that a tunneling-like carriers annihilation may be involved and responsible for the fast fading [39–41].

In the context of the data presented in Figs. 4 and 5 it is noteworthy that the TL peaks recorded during fading experiments are firmly positioned at ~170 °C and ~220 °C. This implies that all the traps (remember about continuous distribution of their energies) generating each of the two TL components decay with essentially similar rate. In turn, this entails that the fading pathways occurs mostly if not exclusively by means of a local process without the use of the host conduction band [42–44], which at room temperature is practically unattainable for trapped electrons, especially those giving rise to the higher-temperature TL. This again brings us to the conclusion that a sort of tunneling is at work in the Lu_2O_3:Tb,V ceramic storage phosphor and causes the very significant fading of TL signal.

Furthermore, right after ceasing the sample irradiation the afterglow shows very low intensity, see Fig. 6b. This denotes that the observed significant fading has mostly non-radiative character [45,46].

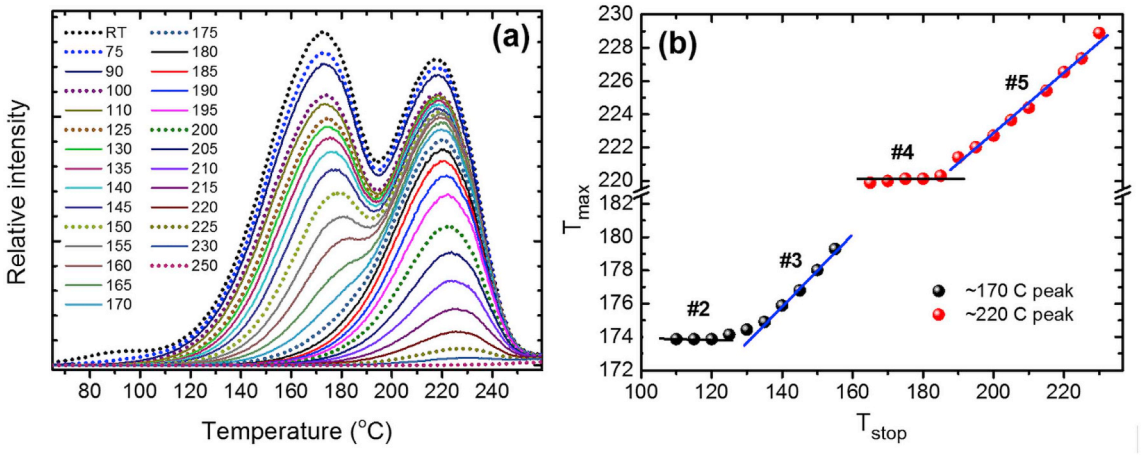

Fig. 5. (a) Glow curves of consecutive TL measurements recorded with increasing T_{stop}. Inset presents values of T_{stop} in °C. (b) T_{max}-T_{stop} dependence derived from the data presented in (a).

Altogether, it appears that fading occurs when electron directly fills the hole immobilized at nearby located Tb and this process does not cause excitation of the dopant to its $^5D_4$ emitting level.

To further trace the thermoluminescence-related processes TL glow curves were recorded varying the heating rate (β) from 1 °C/s to 10 °C/s. The results are presented in Fig. 7. As expected the TL peaks shift to higher temperatures with increasing heating rate [33]. Another clearly seen effect is a continuous increase of the TL intensity with increasing β. This is a rare case described for the first time by Mandowski and Bos [45,47] and later by others [35,40,48]. Recently, analogous effect we observed in Lu_2O_3:Tb,Ta [3].

Mandowski showed that such a situation occurs when regular radiative delocalized TL process competes with a non-radiative one which he termed semi-localized transition (SLT). This theory anticipates profound non-radiative fading and an anomalous dependence of TL intensity on heating rate – exactly as observed in the Lu_2O_3:Tb,V ceramics.

However, SLT mechanism inevitably accelerates the de-trapping process and its characteristic effect is unusually large value of the frequency factor, *s*, related to the trap influenced by the SLT. However, as seen in Table 1, for all the four traps *s* had text-book values for Lu_2O_3. Actually, this does not contradict the SLT mechanism in our case. Namely, the fitting/deconvolution of glow curve peaks was done using two components for each V-related TL peak. As we saw above, see Fig. 5, actually many more traps (of similar depths) contributes to each TL peak. Hence, the parameters of the traps obtained from the fit cannot be taken as real. At most, trap energies obtained from the fit might be considered as very rough estimations of their actual depths, but not the frequency factors, *s*. Hence, the results converge into a consistent picture of processes occurring upon irradiation of the Lu_2O_3:Tb,V ceramics with X-rays and afterwards when natural fading or externally stimulated release of trapped carriers occur.

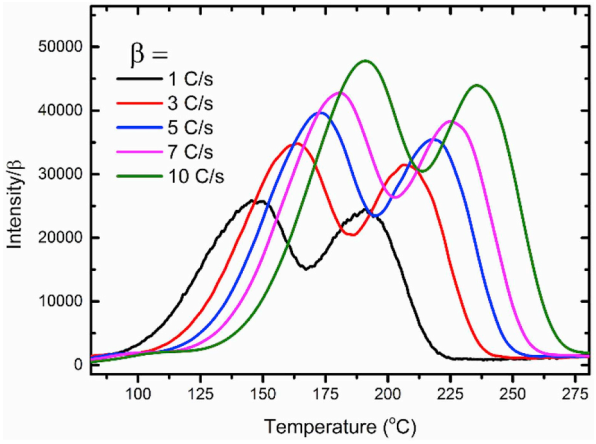

Fig. 7. Heating rate dependence on TL glow curve of Lu_2O_3:0.1%Tb,0.05%V sintered in reducing atmosphere measured after the same X-rays dose. β stands for the heating rate.

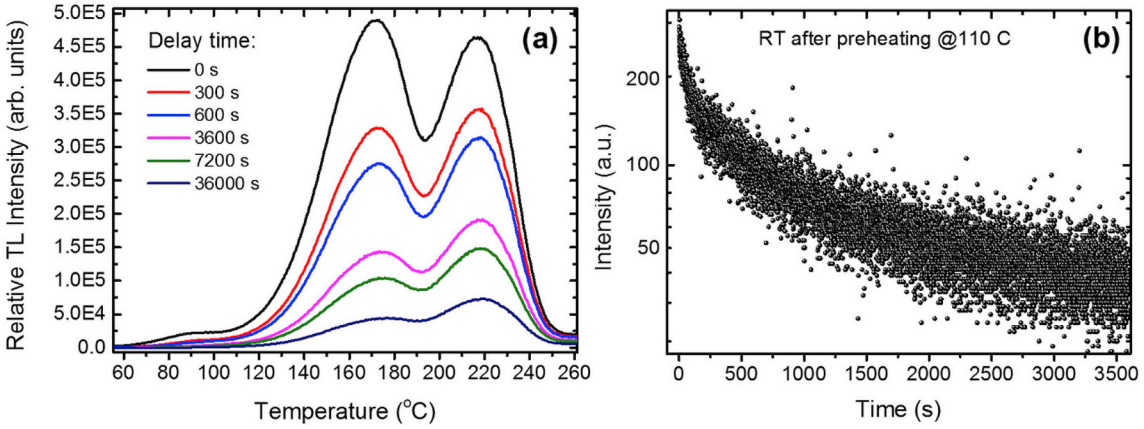

Fig. 6. (a) TL glow curves of Lu_2O_3:0.1%Tb,0.05%V recorded with indicated delay time after irradiation with X-rays. (b) RT decay of afterglow signal after short preheating of the sample up to 110 °C.

4. Conclusions

This paper presents energy storage properties of Lu_2O_3:Tb,V sintered ceramics for the first time. The various processes were traced by a set of complementary thermoluminescent techniques. Two TL peaks around 170 °C and 220 °C were found to directly result from the presence of the V co-dopant. According to the results of previous research on Lu_2O_3:Tb,Ta and along the line with Dorenbos model-the two TL components were assigned to the release of first (170 °C) and second (220 °C) electron from the V-related. Each of the two TL peaks was found to result from a set of traps with some distribution of depths. Supposedly, the distribution is connected with varying distance of the hole- and electron-trapping centers – Tb and V impurities - engaged in the energy storage process. This accords perfectly with the proved contribution from the SLT process to the de-trapping.

There is every reason to accept that, in principle, the carriers trapping occurs according to previously presented schemes for other storage phosphors based on Lu_2O_3:Tb,M. Thus, this is Tb^{3+} which attracts hole and V may immobilize up to two electrons. Their consecutive thermally-stimulated release give rise to the two main TL peaks. What differs the Lu_2O_3:Tb,V from Lu_2O_3:Tb,Ta or Lu_2O_3:Tb,Nb is much lower time-stability of the trapped electrons leading to unexpectedly high fading even from the deepest traps. Anomalous dependence of TL intensity with heating rate – increase of the TL signal when the rate increases – proved that semi-localized transitions occurs in Lu_2O_3:Tb,V. This type of interaction between trapped electrons and holes was also blamed for the substantial and essentially non-radiative fading. This also explains why Lu_2O_3:Tb,V with higher concentration of dopants quickly loose its trapping capability.

Lu_2O_3:Tb,V storage phosphor with its two TL peaks might be interesting for temperature sensing in harsh conditions, as proposed recently [48–50]. Unfortunately, its profound fading is deleterious for such applications. At present, there is no obvious method to deal with this deficiency of the Lu_2O_3:Tb,V storage phosphor, however.

Acknowledgments

The authors gratefully acknowledge financial support by the Polish National Science Centre(NCN) under the grant #UMO-2014/13/B/ST5/01535.

References

[1] E. Zych, Spectroscopy of Eu-activated Lu_2O_3 X-ray phosphors, Front. Semicond. Res, 2006, pp. 1–24.
[2] A. Wiatrowska, E. Zych, Lu_2O_3:Pr,Hf storage phosphor: compositional and technological issues, Materials (Basel) 7 (2014) 157–169, https://doi.org/10.3390/ma7010157.
[3] E. Zych, P. Bolek, D. Kulesza, On thermoluminescence of Lu_2O_3:Tb,Ta ceramic storage phosphors, J. Lumin. 189 (2016) 153–158.
[4] A. Lempicki, C. Brecher, P. Szupryczynski, H. Lingertat, V.V. Nagarkar, S.V. Tipnis, S.R. Miller, A new lutetia-based ceramic scintillator for X-ray imaging, Nucl. Instruments Methods Phys. Res. Sect. A Accel. Spectrometers, Detect. Assoc. Equip. 488 (2002) 579–590, https://doi.org/10.1016/S0168-9002(02)00556-9.
[5] E. Zych, J. Trojan-Piegza, D. Hreniak, W. Strek, Properties of Tb-doped vacuum-sintered Lu_2O_3 storage phosphor, J. Appl. Phys. 94 (2003) 1318–1324.
[6] D. Kulesza, J. Trojan-Piegza, E. Zych, Lu_2O_3:Tb,Hf storage phosphor, Radiat. Meas. 45 (2010) 490–492.
[7] I. Seferis, C. Michail, I. Valais, J. Zeler, P. Liaparinos, N. Kalyvas, G. Fountos, E. Zych, I. Kandarakis, G. Panayiotakis, Imaging performance of a thin Lu_2O_3:Eu nanophosphor scintillating screen coupled to a high resolution CMOS sensor under X-ray radiographic conditions: comparison with Gd_2O_2S:Eu conventional phosphor screen, SPIE Med. Imaging 9033 (2014), https://doi.org/10.1117/12.2042150 90333T.
[8] D. Kulesza, P. Bolek, A.J.J. Bos, E. Zych, Lu_2O_3-based storage phosphors. An (in) harmonious family, Coord. Chem. Rev. 325 (2016) 29–40, https://doi.org/10.1016/j.ccr.2016.05.006.
[9] Y. Guyot, M. Guzik, G. Alombert-Goget, J. Pejchal, A. Yoshikawa, A. Ito, T. Goto, G. Boulon, Assignment of Yb^{3+} energy levels in the C_2 and C_{3i} centers of Lu_2O_3 sesquioxide either as ceramics or as crystal, J. Lumin. 170 (2016) 513–519, https://doi.org/10.1016/j.jlumin.2015.04.017.
[10] M. Guzik, G. Alombert-Goget, Y. Guyot, J. Pejchal, A. Yoshikawa, A. Ito, T. Goto, G. Boulon, Spectroscopy of C_{3i} and C_2 sites of Nd^{3+}-doped Lu_2O_3 sesquioxide either as ceramics or crystal, J. Lumin. 169 (2016) 606–611, https://doi.org/10.1016/j.jlumin.2014.12.063.
[11] S. Kurosawa, L. An, A. Yamaji, A. Suzuki, Y. Yokota, K. Shirasaki, Scintillation Properties of -Doped Ceramics in the Visible and Infrared Regions vol. 61, (2014), pp. 316–319.
[12] V.V. Nagarkar, S.R. Miller, S.V. Tipnis, A. Lempicki, C. Brecher, H. Lingertat, A new large area scintillator screen for X-ray imaging, Nucl. Instrum. Methods Phys. Res. B. 213 (2004) 250–254, https://doi.org/10.1016/S0168-583X(03)01600-8.
[13] C. Brecher, R.H. Bartram, a Lempicki, Hole traps in Lu_2O_3:Eu ceramic scintillators . I . Persistent afterglow, J. Lumin. 106 (2004) 159–168, https://doi.org/10.1016/j.jlumin.2003.09.007.
[14] V.V. Nagarkar, S.V. Tipnis, S.R. Miller, A. Lempicki, C. Brecher, P. Szczupryczynski, H. Lingertat, A new x-ray scintillator for digital radiography, IEEE Trans. Nucl. Sci. 50 (2003) 297–300.
[15] E. Zych, J. Trojan-Piegza, L. Kępiński, Homogeneously precipitated Lu_2O_3:Eu nanocrystalline phosphor for X-ray detection, Sensor. Actuator. B Chem. 109 (2005) 112–118, https://doi.org/10.1016/j.snb.2005.03.006.
[16] J. Trojan-Piegza, E. Zych, J. Hölsä, J. Niittykoski, Spectroscopic properties of persistent luminescence Phosphors : Lu_2O_3:Tb^{3+}, M^{2+} (M= Ca , Sr , Ba), J. Phys. Chem. C 113 (2009) 20493–20498.
[17] J. Trojan-Piegza, J. Niittykoski, J. Hölsä, E. Zych, Thermoluminescence and kinetics of persistent luminescence of vacuum-sintered Tb^{3+} -doped and Tb^{3+} ,Ca^{2+} -co-doped Lu_2O_3 materials, Chem. Mater. 20 (2008) 2252–2261.
[18] D. Kulesza, E. Zych, Managing the properties of Lu_2O_3:Tb,Hf storage phosphor by means of fabrication conditions, J. Phys. Chem. C 117 (2013) 26921–26928.
[19] A. Wiatrowska, E. Zych, Traps formation and characterization in long-term energy storing, J. Phys. Chem. C 117 (2013) 11449–11458.
[20] C.C.S. Pedroso, J.M. Carvalho, L.C.V. Rodrigues, J. Hölsä, H.F. Brito, Rapid and energy-saving microwave-assisted solid-state synthesis of Pr^{3+} -, Eu^{3+} -, or Tb^{3+} -doped Lu_2O_3 persistent luminescence materials, ACS Appl. Mater. Interfaces 8 (2016) 19593–19604.
[21] E. Zych, D. Kulesza, Energy recovery from Lu_2O_3:Tb,Hf ceramic storage phosphors, Zeitschrift Fur Naturforsch. - Sect. B J. Chem. Sci. 69 (2014) 165–170.
[22] P. Dorenbos, Systematic behaviour in trivalent lanthanide charge transfer energies, J. Phys. Condens. Matter 15 (2003) 8417–8434, https://doi.org/10.1088/0953-8984/15/49/018.
[23] P. Dorenbos, Thermal quenching of Eu^{2+} 5d–4f luminescence in inorganic compounds, J. Phys. Condens. Matter 17 (2005) 8103–8111, https://doi.org/10.1088/0953-8984/17/50/027.
[24] A.J.J. Bos, P. Dorenbos, A. Bessière, B. Viana, Lanthanide energy levels in YPO4, Radiat. Meas. 43 (2008) 222–226, https://doi.org/10.1016/j.radmeas.2007.10.042.
[25] P. Dorenbos, Electronic structure engineering of lanthanide activated materials, J. Mater. Chem. 22 (2012) 22344, https://doi.org/10.1039/c2jm34252a.
[26] M. Pechini, Method of preparing lead and alkaline earth titanates and niobates and coating method using the same to form a capacitor, U.S. Pat. No 3,330.697. (1967).
[27] M. Puchalska, P. Bilski, Radiat. Meas. 41 (2006) 659.
[28] Inorganic Crystal Structure Database (ICSD#40471), Fachinformationszentrum Karlsruhe, Germany, 2015.
[29] J. Zeler, L. Jerzykiewicz, E. Zych, Flux-aided synthesis of Lu_2O_3 and Lu_2O_3:Eu—single crystal structure, morphology control and radioluminescence efficiency, Materials (Basel) 7 (2014) 7059–7072, https://doi.org/10.3390/ma7107059.
[30] R. Chen, S.W. McKeever, Theory of Thermoluminescence and Related Phenomena, World Scientific Publishing, 1997.
[31] A.J.J. Bos, Theory of thermoluminescence, Radiat. Meas. 41 (2007) S45–S56, https://doi.org/10.1016/j.radmeas.2007.01.003.
[32] A. Halperin, A.A. Braner, Evaluation of thermal activation energies from glow curves, Phys. Rev. 117 (1960) 408–415, https://doi.org/10.1103/PhysRev.117.408.
[33] S.W.S. McKeever, On the analysis of complex thermoluminescence. Glow-curves: resolution into individual peaks, Phys. Status Solidi 62 (1980) 331–340, https://doi.org/10.1002/pssa.2210620139.
[34] E. Zych, On the reasons for low luminescence efficiency in combustion-made Lu_2O_3:Tb, Opt. Mater. 16 (2001) 445–452, https://doi.org/10.1016/S0925-3467(01)00009-X.
[35] J. Zeler, E. Zych, On the thermoluminescence properties and mechanism of $LuPO_4$:Eu sintered materials, RSC Adv. 6 (2016), https://doi.org/10.1039/c6ra18804d.
[36] W. Drozdowski, K. Brylew, S.M. Kaczmarek, D. Piwowarska, Y. Nakai, T. Tsuboi, W. Huang, Studies on shallow traps in $Li_2B_4O_7$:Eu,Mn, Radiat. Meas. 63 (2014) 26–31, https://doi.org/10.1016/j.radmeas.2014.02.017.
[37] K. Van den Eeckhout, A.J.J. Bos, D. Poelman, P.F. Smet, Revealing trap depth distributions in persistent phosphors, Phys. Rev. B 87 (2013) 1–11, https://doi.org/10.1103/PhysRevB.87.045126.
[38] K. Fiaczyk, A.J. Wojtowicz, W. Drozdowski, K. Brylew, E. Zych, Thermoluminescent properties of HfO_2:Ti after exposure to X-rays, Radiat. Meas. 90 (2016) 140–144, https://doi.org/10.1016/j.radmeas.2016.01.006.
[39] R. Visocekas, A. Zink, Tunneling afterglow and point defects in feldspars, Radiat. Eff. Defect Solid 134 (1995) 265–272, https://doi.org/10.1080/10420159508227228.
[40] A. Dobrowolska, A.J.J. Bos, P. Dorenbos, Electron tunnelling phenomena in YPO_4:Ce,ln (ln = Er, Ho, Nd, Dy), J. Phys. D Appl. Phys. 47 (2014).
[41] I.K. Sfampa, G.S. Polymeris, N.C. Tsirliganis, V. Pagonis, G. Kitis, Prompt isothermal decay of thermoluminescence in an apatite exhibiting strong anomalous fading,

Nucl. Instrum. Methods Phys. Res. Sect. B Beam Interact. Mater. Atoms 320 (2014) 57–63, https://doi.org/10.1016/j.nimb.2013.12.003.
[42] C. Furetta, Questions and Answers on Thermoluminescence (TL) and Optically Stimulated Luminescence (OSL), World Scientific Publishing Co. Pte. Ltd., Singapore, 2008.
[43] S.W.S. McKeever, Thermoluminescence of Solids, Cambridge University Press, Cambridge, U.K, 1985.
[44] S.W.S. McKeever, Optically stimulated luminescence: a brief overview, Radiat. Meas. 46 (2011) 1336–1341, https://doi.org/10.1016/j.radmeas.2011.02.016.
[45] A. Mandowski, A.J.J. Bos, Explanation of anomalous heating rate dependence of thermoluminescence in YPO_4:Ce^{3+},Sm^{3+} based on the semi-localized transition (SLT) model, Radiat. Meas. 46 (2011) 1376–1379, https://doi.org/10.1016/j.radmeas.2011.05.018.
[46] A. Mandowski, A.J.J. Bos, E. Mandowska, J. Orzechowski, Monte-Carlo method for determining the quenching function from variable heating rate measurements, Radiat. Meas. 45 (2010) 284–287, https://doi.org/10.1016/j.radmeas.2009.12.037.
[47] V. Pagonis, L. Blohm, M. Brengle, G. Mayonado, P. Woglam, Anomalous heating rate effect in thermoluminescence intensity using a simplified semi-localized transition (SLT) model, Radiat. Meas. 51–52 (2013) 40–47, https://doi.org/10.1016/j.radmeas.2013.01.025.
[48] M.L. Mah, P.R. Armstrong, S.S. Kim, J.R. Carney, J.M. Lightstone, J.J. Talghader, Thermal history sensing inside high-explosive environments using thermoluminescent microparticles, IEEE Sensors 70 (2011) 1269–1272.
[49] J.J. Talghader, M.L. Mah, E.G. Yukihara, A.C. Coleman, Thermoluminescent microparticle thermal history sensors, Microsystems Nanoeng. 2 (2016) 1–13.
[50] M.L. Mah, M.E. Manfred, S.S. Kim, M. Prokic, E.G. Yukihara, J.J. Talghader, Measurement of rapid temperature profiles using thermoluminescent microparticles, IEEE Sensor. J. 10 (2010) 311–315.